Robust Maximum Power Point Tracking Method for a Stand-Alone PV Power System

Souissi Ahmed[1], Belgacem Ben Ghanem[1], Rebai Najet[1], Hasnaoui Othman[1], Sellami Anis[2]

[1]Unit of research RME, INSAT Tunis, Tunisia
[2]Unit of research C3S, ESSTT, Tunis, Tunisia
Ahmed_souissi@ymail.com

Abstract

This paper proposes a control strategy of a maximum power point of a stand-alone PV system using the sliding mode control technique. This control technique has proved to be very robust with respect to system parameter variations and external disturbances, and provide a simple control law design. The structure selected of the control law is a configuration using the principle of the equivalent and non linear control. The efficiency of the proposed control approach is verified and compared with the traditional P&O technique, through simulations, have shown good performances of the system.

1. Introduction

Recently, the PV system attracted a special interest as a clean energy resource. However, the output density of the PV is low and the power delivered depends highly on the irradiance, temperature, and shadowing conditions. The PV panel has a nonlinear characteristic, and the power has several local maximum power points (MPP) in the I–P characteristic under non-uniform insolation; thereby MPP tracking should be used to track its changes.

Many MPP tracking techniques have been reported in the literature for tracking the optimal operating point, in order to extract the maximum energy from the PV modules. The reference [1] grouped these methods on three classes: the indirect control, the direct control and the artificial intelligence methods. Some of these, with their advantages and disadvantages, are recapitulated in [1, 2].

In this paper, a developed sliding mode control strategy is applied to maximize the power extracted from the PV module. This control technique has proved to be very robust with respect to system parameter variations and external disturbances. Other recent example of sliding mode utilized for PV control applications can be found in [3-5].

This paper is organized as follows: the first section describe the PV characteristic. The second one gives the non linear model of the system. Then, the sliding mode control approach is given in the third section. Finally, simulations results are used to illustrate the validity of the proposed approach.

2. PV Characteristic

The solar panel used in this work is one of a ten panels installed on the roof of the laboratory research unit (RME) at INSAT. It has a rated power of 50W.

The electrical behaviour of the photovoltaic cell may be simply modelled by a nonlinear current source connected in series with the intrinsic cell series resistance. The characteristic equation for the current and voltage of a PV array conducts as a function of solar irradiance and cell temperature is described as follows [6, 7]

$$i_{pv} = n_p I_{ph} - n_p I_{rs}\left(e^{q\left(v_{pv}+i_{pv}R_s\right)/n_s AKT} - 1\right) \quad (1)$$

In which i_{pv} is the PV array output current, v_{pv} is the PV array output voltage, n_p represents the number of parallel modules, each one is constituted by n_p cells connected in series, q is the electronic charge, K is Boltzmann's constant, T is the cell temperature in Kelvin, E is the insolation in mW/cm^2 and A is the ideal p−n junction factor. The cell reverse saturation current I_{rs} and the photocurrent I_{ph} are given by the following expressions:

$$I_{rs} = I_{or}\left(\frac{T}{T_r}\right)^3 e^{qE_{go}\left(\frac{1}{T_r}-\frac{1}{T}\right)/KT} \quad (2)$$

$$I_{ph} = \left(I_{sc} + K_I\left(T - T_r\right)\right)E/100 \quad (3)$$

Where I_{or} is the reverse saturation current at the reference temperature T_r, E_{go} is the band-gap energy of the semiconductor, I_{sc} is the short-circuit cell current at reference temperature and insolation, and K_I is the short-circuit current temperature coefficient.

The PV cell temperature is given by the following equation [8]:

$$T = \frac{T_a + \left(T_{c,NOCT} - T_{a,NOCT}\right)\left(\frac{G_T}{G_{T,NOCT}}\right)\left[1 - \frac{\eta_{mp,STC}\left(1-\alpha_p T_{c,STC}\right)}{\tau\alpha}\right]}{1 + \left(T_{c,NOCT} - T_{a,NOCT}\right)\left(\frac{G_T}{G_{T,NOCT}}\right)\left(\frac{\alpha_p \eta_{mp,STC}}{\tau\alpha}\right)} \quad (4)$$

Where T_a is the ambient temperature, $T_{c,NOCT}$ is the nominal operating cell temperature, $T_{a,NOCT}$ is the ambient temperature at which the NOCT is defined (20°C), $G_{T,NOCT}$ is the solar radiation at which the NOCT is defined (0.8 kW/m2), τ is the solar transmittance of any cover over the PV array (%), α is the solar absorptance of the PV array (%), the product of the solar absorptance and the solar transmittance is 0.9 or 90%, and $\eta_{mp,STC}$ is the MPP efficiency under standard test conditions, it is given by:

$$\eta_{mp,STC} = \frac{Y_{pv}}{A_{pv} G_{T,STC}} \tag{5}$$

Where A_{pv} is the surface area of the PV module (m^2), $G_{T,STC}$ is the incident radiation at standard test conditions (1 kW/m²) and Y_{pv} is the rated capacity of the PV panel (kW).

Figure 1 shows the dependence of a typical current versus voltage characteristic on solar irradiation and temperature.

For radiation varying between 40mW/cm^2 and 80mW/cm^2, we obtain experimental characteristics $i_{pv} = f(v_{pv})$ for a temperature between 15°C and 16°C (black curve) and for a temperature between $31°C$ and $33°C$ (blue curve in dotted line), Figure 1. These characteristics have been reported in December 2009 and on July 2010.

We note that the solar irradiance has preeminent influence on the short-circuit current unlike the open circuit voltage remains virtually constant.

The temperature increase has a negative influence on the energy supplied by the panel. The open-circuit voltage decreases with increasing temperature. This voltage reduction causes consequently a decrease of power.

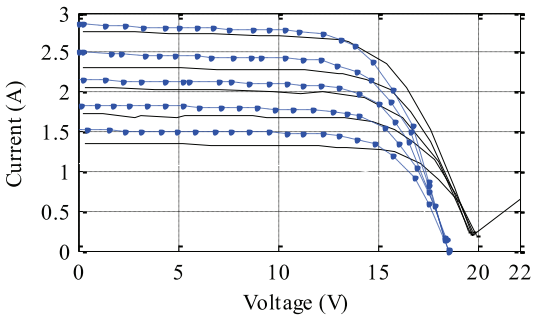

Fig. 1. PV characteristic under different irradiance levels and under different temperature

3. System modeling

The stand-alone PV power system adopted in this study is shown in Figure 2. It's constituted by a PV module, a DC/DC buck converter and a battery bank. The DC/DC converter is used to increase the efficiency of the system by controlling, indirectly, the operation point of the PV module. Through adjusting the duty cycle of the converter, we can thus regulate the PV module output voltage to the MPP and, therefore, affects the output power of the PV array module.

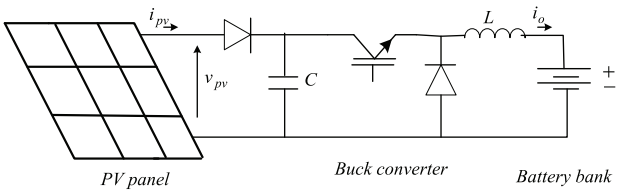

Fig. 2. Structure of the stand-alone PV system

The stand-alone PV system dynamic equation can be expressed as follows:

$$\begin{aligned} \dot{v}_{pv} &= \frac{i_{pv}}{C} - \frac{i_o}{C} u \\ \dot{i}_o &= -\frac{v_b}{L} + \frac{v_{pv}}{L} u \end{aligned} \tag{6}$$

Where i_o and v_b are the current and voltage at the output terminals of the buck converter, u is the duty ratio.

Modeling the battery bank as a voltage source E_b connected in series with a resistance R_b and a capacitor C_b [9]. The voltage on the dc bus terminals is given by:

$$v_b = E_b + v_c + R_b i_o \tag{7}$$

v_c is the voltage on C_b .

A complete nonlinear dynamical model of the stand-alone PV system may be written as:

$$\dot{x} = F(x,t) + G(x,t)u(t) \tag{8}$$

Where $x = \left[v_{pv}\ i_o\ v_c \right]$; $F(x,t) = \left[\frac{i_{pv}}{C}\ \frac{-v_b}{L}\ \frac{i_o}{C_b} \right] = \left[A1\ A2\ A3 \right]$

and $G(x,t) = \left[-\frac{i_o}{C}\ \frac{v_{pv}}{L}\ 0 \right] = \left[B1\ B2\ B3 \right]$

The stand-alone PV system has a nonlinear characteristic, and the power has a MPP at a certain working point. The control law adopted in this study to track the maximum power from the PV panel is based on the sliding mode control approach.

4. Sliding mode control approach

The sliding mode control consists in bringing the trajectory of state of the considered system towards a sliding surface. When the state is maintained on this surface, the system is in sliding mode, its dynamics is then insensitive to some classes of external disturbances and parameter variations as long as the conditions of the sliding mode are assured.

The implementation of this method of control requires mainly three steps:

- selecting the sliding surface $s(x,t) = 0$ (where x is the system's state vector).
- guarantying the condition of convergence towards the sliding surface which called reaching condition. It's given by:

$$s(x)\dot{s}(x) \prec 0 \tag{9}$$

- designing the control law

Before beginning the design of the sliding mode control law, we will synthesize the sliding surface. As the principal goal is to track the MPP of the PV panel, the condition of the MPP is given by:

$$\frac{\partial P_{pv}}{\partial v_{pv}} = \frac{\partial\left(i_{pv}\left(v_{pv}\right)v_{pv}\right)}{\partial v_{pv}} = \frac{\partial i_{pv}}{\partial v_{pv}}v_{pv} + i_{pv} = 0 \qquad (10)$$

The sliding surface must be:

$$s(x) = \frac{\partial i_{pv}}{\partial v_{pv}}v_{pv} + i_{pv} \qquad (11)$$

Based on the observation of duty cycle versus PV power and sliding surface as depicted in Figure 3, the sliding surface is negative for higher duty cycle and positive for lower duty cycle.

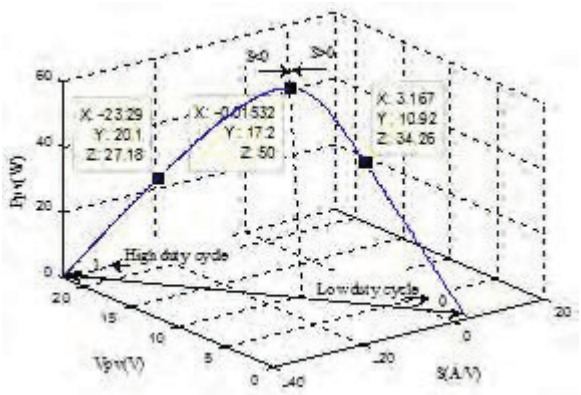

Fig. 3. Evolution of sliding surface versus duty cycle

The control law selected is a configuration using the principle of the equivalent u_{eq} and non linear control u_n :

$$u(t) = u_{eq} + u_n \qquad (12)$$

The equivalent component is calculated by assuming that the behavior of the system during the sliding mode is described by:

$$\dot{s}(x) = 0 \qquad (13)$$

The equivalent control can be given by [10]:

$$u_{eq}(t) = -\left[\left[\frac{\partial s}{\partial x}\right]G(x,t)\right]^{-1}\frac{\partial s}{\partial x}F(x,t) \qquad (14)$$

The dynamics of the system during the sliding mode are given as follows:

$$\dot{x} = \left[I - G(x,t)(\frac{\partial s}{\partial x}G(x,t))^{-1}(\frac{\partial s}{\partial x})\right]F(x,t) \qquad (15)$$

The non linear component u_n is given to guarantee the reaching condition. It is given by [11]:

$$u_n = -k|s|^{\sigma}\, sign(s) \qquad (16)$$

Where: $0 < \sigma < 1$ and $k \succ 0$

After development, the expression of the equivalent component is given by:

$$u_{eq} = -\left[\frac{\partial s}{\partial v_{pv}}B1\right]^{-1}(\frac{\partial s}{\partial v_{pv}}A1) = \frac{i_{pv}}{i_o} \qquad (17)$$

Since the range of duty cycle is between 0 and 1, the final control law is given by:

$$u = \begin{cases} 1 & u_{eq} - k|s|^{\sigma}\, sign(s) \geq 1 \\ u_{eq} - k|s|^{\sigma}\, sign(s) & \text{for } 0 \prec u_{eq} - k|s|^{\sigma}\, sign(s) \prec 1 \\ 0 & u_{eq} - k|s|^{\sigma}\, sign(s) \leq 0 \end{cases} \qquad (18)$$

The proposed control law is composed by u_{eq} and u_n, where u_{eq} is the required effort to remain on the sliding surface and u_n can be considered as the effort to track the MPP. To guarantee the existence of the MPP state $s = 0$ using the proposed control law, the reaching condition defined by equation (9) must be verified:

- For $1 \prec u \prec 0$

$$s\dot{s} = s\frac{\partial s}{\partial v_{pv}}\dot{v}_{pv} \qquad (19)$$

$$\frac{\partial i_{pv}}{\partial v_{pv}} = -n_p I_{rs}\frac{q}{n_s AKT}(e^{q\left(v_{pv}+i_{pv}R_s\right)/n_s AKT}) \prec 0 \qquad (20)$$

$$\frac{\partial s}{\partial v_{pv}} = \frac{\partial i_{pv}}{\partial v_{pv}}\left(2 + v_{pv}\frac{q}{n_s AKT}\right) \prec 0 \qquad (21)$$

$$\begin{aligned} \dot{v}_{pv} &= A1 + B1\cdot u = A1 + B1\cdot\left(u_{eq} + u_n\right) \\ &= B1\cdot u_n = \frac{i_o}{C}k|s|^{\sigma}\, sign(s) \end{aligned} \qquad (22)$$

Based on the result of (21) and (22):

$$s\dot{s} = s\frac{\partial s}{\partial v_{pv}}\cdot\frac{i_o}{C}k|s|^{\sigma}\, sign(s) \prec 0 \qquad (23)$$

Therefore, $s\cdot\dot{s} \prec 0$ for $1 \prec u \prec 0$.

- For $u = 0$

$$\dot{v}_{pv} = A1 = \frac{i_{pv}}{C} \succ 0 \qquad (24)$$

By (21) and (24), $\dot{s} \prec 0$

We can see from Figure 3, the sliding surface is positive for lower duty cycle.

Therefore, $s\cdot\dot{s} \prec 0$ for $u = 0$.

- For $u = 1$

$$\dot{v}_{pv} = A1 + B1 = \frac{i_{pv}}{C} - \frac{i_o}{C} \prec 0 \qquad (25)$$

By (21) and (25), $\dot{s} \succ 0$

We can see from Figure 3, the sliding surface is negative for higher duty cycle.

Therefore, $s\cdot\dot{s} \prec 0$ for $u = 1$.

Finally, the reaching condition towards the sliding surface is verified and the existence of the MPP state $s = 0$ using the proposed control law is guaranteed.

5. Simulation results

In order to verify the efficiency of the proposed sliding mode controller and compare it with one of the most commonly used algorithm, P&O technique, computer simulations were conducted using the parameters shown in Table 1.

Table 1. Parameters for simulation

n_p	1
n_s	36
T_r	301.18 K
E_{go}	1.1 V
K	1.38 10^-23 Nm/K
A	1.6
I_{or}	2.6993 10^-6 A
E_b	12 V
q	1.602 10^-19 C
R_b	0.018 Ω
C	0.00001 F
L	0.006 H
k	0.4
σ	0.89

P&O technique is an iterative method of searching MPP. It measures the PV panel characteristics (current, voltage and power) at every moment, and then perturbs the operating point of PV panel while adjusting directly on the duty cycle of the DC-DC converter. After that, one observes his effect on the power delivered by PV panel: If a given perturbation leads to an increase (decrease) in the PV power, the following perturbation is made in the same (opposite) direction.

Figure 4 and 5 shows the evolution of irradiation and the PV cell temperature used in the simulation. It's varying respectively between 40 and 100 mW/cm2, and 15 and 32°C.

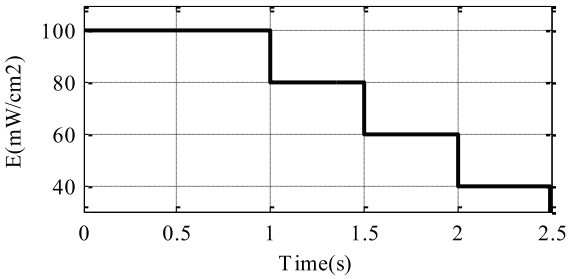

Fig. 4. Insolation profile

Figure 6 and 7 presents respectively the current and voltage delivered by the PV panel using the sliding mode control and the P&O technique.

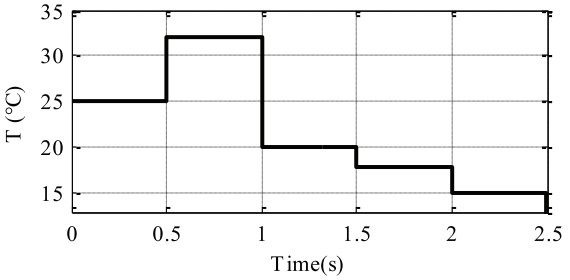

Fig. 5. PV panel temperature

Figures 9 and 10 respectively show the evolution of the duty cycle and power delivered by the PV panel with the sliding mode (black curve) and the P&O technique (blue curve). It is observed that the PV current decreases linearly with decrease in irradiation value.

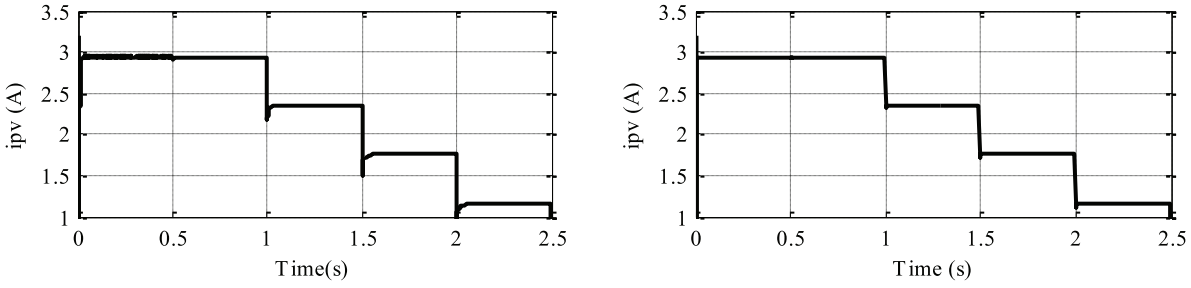

–a) the P&O technique -b) the sliding mode

Fig. 6. PV panel output current with:

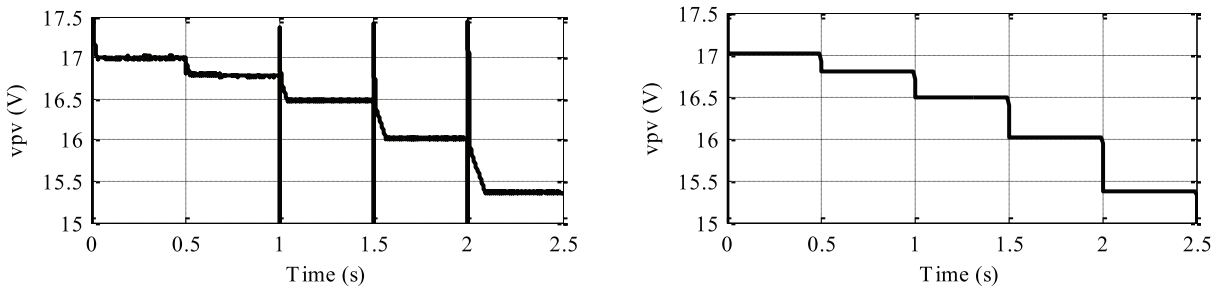

–a) the P&O technique -b) the sliding mode

Fig. 7. PV panel output voltage with:

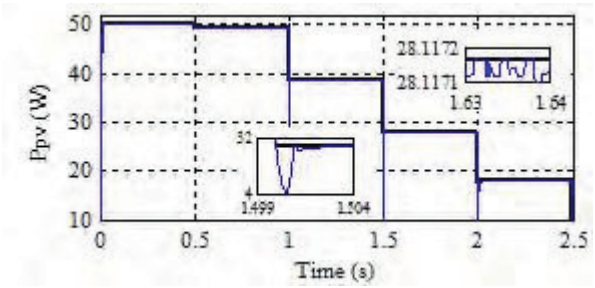

Fig. 8. PV panel output power

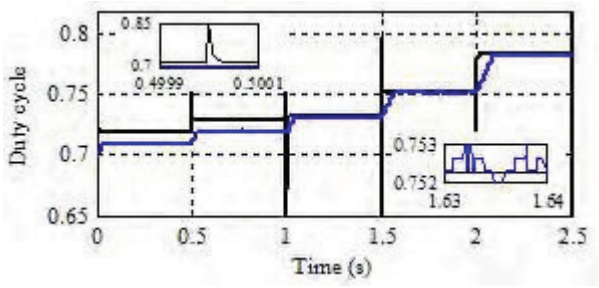

Fig. 9. Duty cycle control signal

The temperature increase has a negative influence on the power delivered by the panel. Indeed, at t=0.5s, an increase of temperature for a constant irradiation equal to 100mW/cm2 caused a remarkable decrease of voltage unlike the PV current remains virtually constant.

With the P&O technique, it is clear that the PV power oscillates around the maximum power point even though the irradiation and temperature are constant; causing a power loss, figure 8. Furthermore, when a sudden decrease in insulation, the traditional P&O get confused, as it cannot interpret correctly the change in power caused by the irradiation. It reacts in a wrong direction moving it away from the optimal point until he returns oscillates around the maximum power point, a time after the stability of the irradiation.

In against part, the sliding mode control is robust to rapidly changing climatic conditions and its response time is fast.

The sliding surface is practically equal to zero, Figure 10, which implies the effectiveness and the robustness of the sliding control law to track the maximum power operation point in spite of the rapid changes in the atmospheric condition.

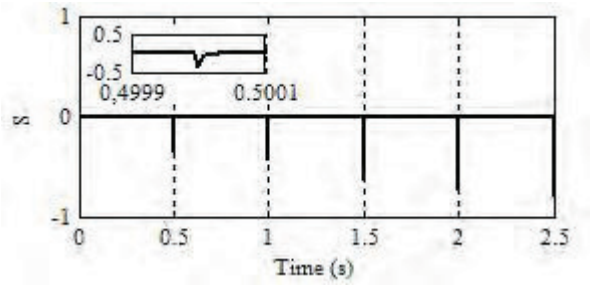

Fig. 10. Evolution of the sliding surface

6. CONCLUSION

A sliding mode control approach of a maximum power operation point of a stand-alone photovoltaic system has been developed in this paper. The proposed control law is a configuration using the principle of the equivalent and non linear control. The sliding surface selected is based on the conductance incremental method by differentiating the PV power with respect to voltage and setting the result to zero.

The proposed control approach has been compared with the P&O technique to prove its efficiency and robustness against the variations of the atmospheric conditions.

7. REFERENCES

[1] V. Salas, E. Olias, A. Barrado and A. Lazaro, "Review of the maximum power point tracking algorithms for stand-alone photovoltaic systems", *Solar Energy Materials & Solar Cells,* vol. 90, no. 11, pp. 1555-1578, 2006.

[2] D. Sera, T. Kerekes, R. Teodorescu and F. Blaabjerg, "Improved MPPT algorithms for rapidly changing environmental conditions", *Power Electronics and. Motion Control Conference*, Portoroz, 2006, vol. 4, pp. 1614-1619.

[3] H. De Battista, and R.J. Mantz, "Variable structure control of a photovoltaic energy Converter", *IEE Proc. Control Theory Appl.*, vol. 149, no. 4, pp. 303-310, 2002.

[4] C-C Chu and C-L Chen, "Robust maximum power point tracking method for photovoltaic cells: A sliding mode control approach", *Solar Energy*, vol. 38, no. 8, pp. 1555-1578, 2009.

[5] F. Valenciaga, and P.F. Puleston, "Supervisor Control for a Stand-Alone Hybrid Generation System Using Wind and Photovoltaic Energy", *IEEE Trans. Energy Convers.*, vol. 20, no. 2, pp. 398-405, 2005.

[6] K.H. Hussein, I. Muta, T. Hoshino and M. Osakada, "Maximum photovoltaic power tracking: an algorithm for rapidly changing atmospheric condition", *IEE Proc. Gener., Transm. Distrib.*, vol.45, no.1, pp. 59-64, 1995.

[7] R. Kyoungsoo, and S. Rahman, "Two-loop controller for maximizing performance of a grid-connected photovoltaic-fuel cell hybrid power plant", *IEEE Trans. Energy Convers.,* vol. 13, no. 3, pp. 276-281, 1998.

[8] Help files of the software Homer, V2.68 beta: National Renewable Energy Laboratory (NREL), 617 Cole Boulevard, Golden, CO 80401-3393. Available: http://www.nrel.gov/homer

[9] B.S. Borowy and Z.H. Salameh, "Dynamic response of a standalone wind energy conversion system with battery energy storage to a wind gust", *IEEE Trans. Energy Convers.,* vol. 12, no. 1, pp. 73-78, 1997.

[10] J. J. E. Slotine and W. Li, "Applied Nonlinear Control", Prence Hall, USA, 1998.

[11] Gao and James C. Hung, "Variable Structure Control of Nonlinear Systems: A New Approach", *IEEE Trans. Ind. Elec.*, vol. 40, n°1, Feb 1993.